

Penumbra Detection in Acute Stroke with Perfusion Magnetic Resonance Imaging: Validation with ^{15}O -Positron Emission Tomography

Olivier Zaro-Weber, MD,^{1,2,3} Hermann Fleischer,^{1,2,3} Lucas Reiblich,^{1,2,3}

Alexander Schuster, BSc,¹ Walter Moeller-Hartmann, MD,⁴ and Wolf-Dieter Heiss, MD¹

Objective: Accurate identification of the ischemic penumbra, the therapeutic target in acute clinical stroke, is of critical importance to identify patients who might benefit from reperfusion therapies beyond the established time windows. Therefore, we aimed to validate magnetic resonance imaging (MRI) mismatch-based penumbra detection against full quantitative positron emission tomography (^{15}O -PET), the gold standard for penumbra detection in acute ischemic stroke.

Methods: Ten patients (group A) with acute and subacute ischemic stroke underwent perfusion-weighted (PW)/diffusion-weighted MRI and consecutive full quantitative ^{15}O -PET within 48 hours of stroke onset. Penumbra as defined by ^{15}O -PET cerebral blood flow (CBF), oxygen extraction fraction, and oxygen metabolism was used to validate a wide range of established PW measures (eg, time-to-maximum [Tmax]) to optimize penumbral tissue detection. Validation was carried out using a voxel-based receiver-operating-characteristic curve analysis. The same validation based on penumbra as defined by quantitative ^{15}O -PET CBF was performed for comparative reasons in 23 patients measured within 48 hours of stroke onset (group B).

Results: The PW map Tmax (area-under-the-curve = 0.88) performed best in detecting penumbral tissue up to 48 hours after stroke onset. The optimal threshold to discriminate penumbra from oligemia was Tmax >5.6 seconds with a sensitivity and specificity of >80%.

Interpretation: The performance of the best PW measure Tmax to detect the upper penumbral flow threshold in ischemic stroke is excellent. Tmax >5.6 seconds-based penumbra detection is reliable to guide treatment decisions up to 48 hours after stroke onset and might help to expand reperfusion treatment beyond the current time windows.

ANN NEUROL 2019;85:875–886

The ischemic penumbra was defined by Astrup and colleagues in 1981 as the condition of ischemic brain perfused at a level of functional impairment (ie, electric failure) but persistent cellular integrity, which has the potential to recover if perfusion is improved.¹ Identification of the ischemic penumbra has therefore been of critical importance to guide reperfusion therapies of ischemically compromised but viable brain tissue in acute ischemic stroke.^{2,3} The time-dependent viability of the ischemic penumbra,

with the ischemic core expanding into the surrounding penumbra if no reperfusion is achieved, emphasizes the need for a rapid and valid detection of penumbral tissue in the clinical setting.^{4,5}

Various imaging modalities have been applied to detect penumbral tissue in acute ischemic stroke. In clinical stroke, the oxygen-15 positron emission tomography (^{15}O -PET) technique was the first to image penumbra in vivo. Penumbral tissue was defined by a reduced cerebral blood flow

View this article online at wileyonlinelibrary.com. DOI: 10.1002/ana.25479

Received Nov 2, 2018, and in revised form Mar 20, 2019. Accepted for publication Mar 31, 2019.

Address correspondence to Dr Zaro-Weber, Max Planck Institute for Neurological Research, Gleueler Str 50, 50931 Cologne, Germany.
E-mail: zaroweber@nf.mpg.de

H.F. and L.R. contributed equally.

From the ¹Max Planck Institute for Neurological Research, Cologne; ²Department of Neurology, Charité-Universitätsmedizin Berlin, Berlin; ³Center for Stroke Research Berlin, Charité-Universitätsmedizin Berlin, Berlin; and ⁴Department of Radiology and Neuroradiology, University Hospital Cologne, Cologne, Germany

(CBF) with an elevated oxygen extraction fraction (OEF) accounting for a proportionally preserved or even normal cerebral metabolic rate of oxygen (CMRO₂).^{4,6–11} Although PET is still considered the gold standard for penumbra detection in acute human stroke,^{2,3} it requires complex logistics and is difficult to perform in the clinical setting. Therefore, simpler and wider applicable imaging modalities to detect penumbral tissue in acute ischemic stroke, such as the mismatch concept in magnetic resonance imaging (MRI), have been introduced.^{12,13} Since the first operational definition of the MRI-based “mismatch” between diffusion-weighted (DWI) and perfusion-weighted (PWI) MRI as a surrogate of penumbra in acute stroke,¹⁴ the mismatch concept is still challenged by the accurate PWI-based discrimination of penumbral from oligemic tissue to select candidates for therapeutic interventions.

To optimize the detection of tissue at risk of infarction based on PWI, various perfusion maps and their corresponding thresholds have been investigated. In the clinical setting, however, the choice of the best PW map and its optimal upper penumbral flow threshold is still a matter of debate.¹⁵ To address this controversy, and because recent stroke studies have proven for the first time the clinical benefit of mismatch-based thrombectomy 6 to 24 hours after stroke onset (DEFUSE-3, DAWN),^{16,17} it is important to validate PW parameters with full quantitative ¹⁵O-PET to make this imaging procedure a reliable tool to detect salvageable tissue in acute stroke. Several previous studies validated PW maps in terms of tissue at risk detection in acute stroke against absolute or relative CBF measures (PET, single photon emission computed tomography, and xenon computed tomography [Xe-CT]).¹⁵ However, flow measures alone, even though established, are only surrogate markers to define penumbral tissue. Therefore, we validated the mismatch concept against the classic concept of penumbra as defined by full quantitative ¹⁵O-PET measures of blood flow and oxygen metabolism (PET-CBF, -OEF, and -CMRO₂). In addition, to give a more complete image of the optimal PWI maps and thresholds to detect the penumbral flow threshold, we also validated PWI map performance based on our bigger quantitative PET-CBF group for comparative reasons.

To help clinicians assess the tissue at risk of infarction with high accuracy, we validated for the first time a wide range of PWI maps up to 48 hours after stroke against full quantitative ¹⁵O-PET in terms of (1) their threshold independent performance to detect the penumbral flow threshold, (2) their best threshold to optimize the detection of the penumbral flow threshold, and (3) their performance to detect the penumbral flow threshold up to 48 hours after stroke onset.

Patients and Methods

Patients

This study includes 2 different groups of patients with acute and subacute ischemic hemispheric stroke. Group A was measured with full quantitative ¹⁵O-PET to evaluate CBF, cerebral blood volume (CBV), OEF, and CMRO₂; group B was measured with quantitative ¹⁵O-PET to evaluate CBF. These patients underwent acute consecutive MRI and PET within 48 hours of symptom onset as part of a prospective research protocol. The comparative PET-MRI patient sample (PET-MR validation group) was measured on the same scanners with the same procedures and sequences. The patients in group A were studied from 2004 to 2017. Four patients have previously been reported, but these studies either had another focus or were methodically different or both.^{18–21,29} The patients in group A were selected from our PET-MR validation group based on full quantitative ¹⁵O-PET CBF, OEF, and CMRO₂ measured within 48 hours of stroke onset. The patients in group B were studied from 2003 to 2016. All have previously been reported, but these studies either had another focus or were methodically different or both.^{18,19,21–23} The patients in group B were selected from our PET-MR validation group based on quantitative ¹⁵O-PET CBF measured within 48 hours of stroke onset. The patients in group B were analyzed in line with group A and included in the study for comparative reasons. An experienced stroke neurologist supervised the patients during the whole procedure according to our stroke unit standards, and only clinically stable patients were included in the study. Time between both imaging modalities was kept as short as possible (for time intervals, see clinical data in the Results section), and patients with clinical changes in National Institutes of Health Stroke Scale (NIHSS) >2 during and between both imaging procedures were excluded. Patients receiving thrombolytic therapy or thrombectomy did not receive PET after MRI and were not included in the study. The study was approved by the local ethics committee of the University of Cologne, Germany. All patients gave written informed consent in accordance with the ethical standards of the Helsinki Declaration of 1975 and its later amendments.

MRI and PET Image Acquisition

MRI was performed in both groups on a 1.5T whole-body scanner (Intera Master; Philips, Best, the Netherlands). Dynamic susceptibility contrast (DSC) PWI was performed in an axial direction (20 slices, slice thickness = 6mm, interslice gap = 0.6mm, field of view = 23cm), and multishot 3-dimensional (3D) T2*-weighted gradient echoplanar imaging (EPI) sequences (principles of echo shifting using a train of observations; effective echo time [TE] = 25 milliseconds, flip angle = 9°, EPI factor = 17, matrix = 64 × 51, resulting voxel size = 3.6 × 3.6 × 6mm) were used. The DSC PW protocol

included 60 measurements at intervals of 1.3 seconds after standardized intravenous injection of 20ml of gadolinium-diethylenetriaminepentaacetic acid (Magnevist, Schering AG; power-injector flow rate 10ml/s, followed by 20ml saline). DWI used single shot spin-echo EPI (TE = 96 milliseconds, repetition time = 3,560 milliseconds, flip angle = 90°, matrix = 256 × 256, field of view [FoV] = 230 × 230, b = 0 and b = 1,000, pixel size = 0.9 × 0.9mm², slice thickness = 6mm, interslice gap = 0.6mm), and T1 fast field echo (FFE) sequence was TE = 1.8 milliseconds, TR = 145 milliseconds, flip angle = 80°, matrix = 256 × 256, FoV = 230 × 230, pixel size = 0.9 × 0.9mm², slice thickness = 6mm, interslice gap = 0.6mm.

PET was performed in a resting state on an ECAT EXACT HR scanner (CTI; Siemens, Erlangen, Germany). Emission scans were performed in a 2- and 3D data acquisition mode providing 47 contiguous 3mm slices of 5mm full width at half maximum (FWHM) in plane reconstructed resolution.²⁴ The PET investigations of group A consisted of a total of 3 studies, with the complete study lasting approximately 30 to 40 minutes.²⁵ CBF was measured with an intravenous bolus of 60mCi (2.2GBq) ¹⁵O-H₂O.²⁶ OEF was measured with ¹⁵O-O₂ gas inhaled by a deep single breath of 50mCi (1.85GBq) followed by breath holding of approximately 10 to 15 seconds.²⁵ CBV was measured by inhalation of 50mCi (1.85GBq) ¹⁵O-CO allowing equilibrium before PET scanning was started.²⁷ For both ¹⁵O-H₂O and ¹⁵O-O₂ measures, an arterial input function (AIF) was measured by continuous arterial blood sampling (radial artery) with an automated blood-sampling system.²⁸ For the ¹⁵O-CO studies, manually drawn blood samples were measured in a well counter after equilibrium between brain and blood activities was reached. From these measures, regional values of CBF, CBV, OEF, and CMRO₂ were generated on a pixel-by-pixel basis as described previously.²⁵ For details, see Heiss and colleagues⁴ and Sobesky and colleagues.²⁹ The PET investigations of group B consisted of 1 study of quantitative PET-CBF, with the complete study lasting approximately 10 minutes.²⁵

All further postprocessing and analysis of the data from group B, which validated PWI maps based only on the established PET-CBF penumbra threshold, were performed in line with group A.

MRI Postprocessing

Postprocessing of the MRI DSC PW raw images was performed by using our in-house software to realign all raw Digital Imaging and Communications in Medicine (DICOM) DSC PW images to correct for movement artifacts.³⁰ Then we used the research software PMA (v5.0)³¹ to generate (1) the nondeconvolved PW maps time to peak (TTP), bolus arrival time (BAT), bolus end time (BET), FWHM, first moment (FM) without delay correction (DC), FM with DC, CBV of

the curve of the tissue contrast time curve (CBV_{CTC}), maximum concentration (C_{max}), negative enhancement integral (NEI), normalized signal drop (dS/S) and maximum slope (MS) of the tissue response curve before deconvolution; and (2) the deconvolved PW maps CBF, CBV, mean transit time (MTT), and time to maximum (T_{max}; Fig 1). Deconvolved PW maps were derived from the deconvolved tissue response curve using the nonparametric standard singular value decomposition method.³² Deconvolution was performed with a nondistorted AIF defined by 5 to 10 voxels manually chosen from the contralateral proximal M1 segment of the middle cerebral artery (MCA).²¹ For a detailed description of these maps calculated with PMA, see the study by Leiva-Salinas and colleagues.³³

Normalization of the nondeconvolved PW maps (eg, to remove variability due to injection timing and arrival time differences of the bolus contrast agent) was performed in line with previous studies.^{21,34} For this purpose, the mean value of a region of interest (ROI) covering the MCA territory contralateral to the affected hemisphere, in a slice including the basal ganglia, was determined. All temporal PWI parameters (eg, TTP, FM, BAT, BET, and FWHM) were normalized by subtraction of the mean contralateral ROI value (eg, TTP_{absolute} - TTP_{ROI}). Normalization of nondeconvolved surrogates of CBF and CBV (eg, C_{max}, MS, and CBV_{CTC}) were expressed as the ratio to the contralateral mean ROI value (eg, C_{max}_{absolute} / C_{max}_{ROI}).^{34,35}

MRI and PET Image Analysis

All PET and MR images were analyzed with a multimodal-imaging tool VINCI (Max Planck Institute for Neurological Research, Cologne, Germany). To match spatial resolution, PET images were resized to the PW MR images, which were previously filtered (gauss 3D filter) to match the FWHM of the PET images. All PET and MR images were then realigned by a fully automated algorithm.³⁰ For each patient, a 3D grey matter brain mask based on the individual T1 image was automatically created and manually corrected using VINCI. The grey matter masks were resliced to the PW MR image dimensions. Then a direct voxel-based analysis of the PET and MR images was performed within this individual 3D brain mask including the cortex (grey matter) of the ischemic hemisphere. The voxel values from the coregistered PET-CBF, -CBV, -OEF, -CMRO₂ and PW-MRI maps (group A) and PET-CBF and PW-MRI maps (group B) were used for a direct voxel-based analysis. PET CBV voxels >8.0ml/100g/min were excluded as artifactual (group A).³⁶ Voxels within the infarcted tissue without contrast bolus arrival during PWI scanning were excluded from further analysis.³⁷ To prevent our analysis from being biased by necrosis or established reperfusion (very low OEF), we excluded all voxels with OEF

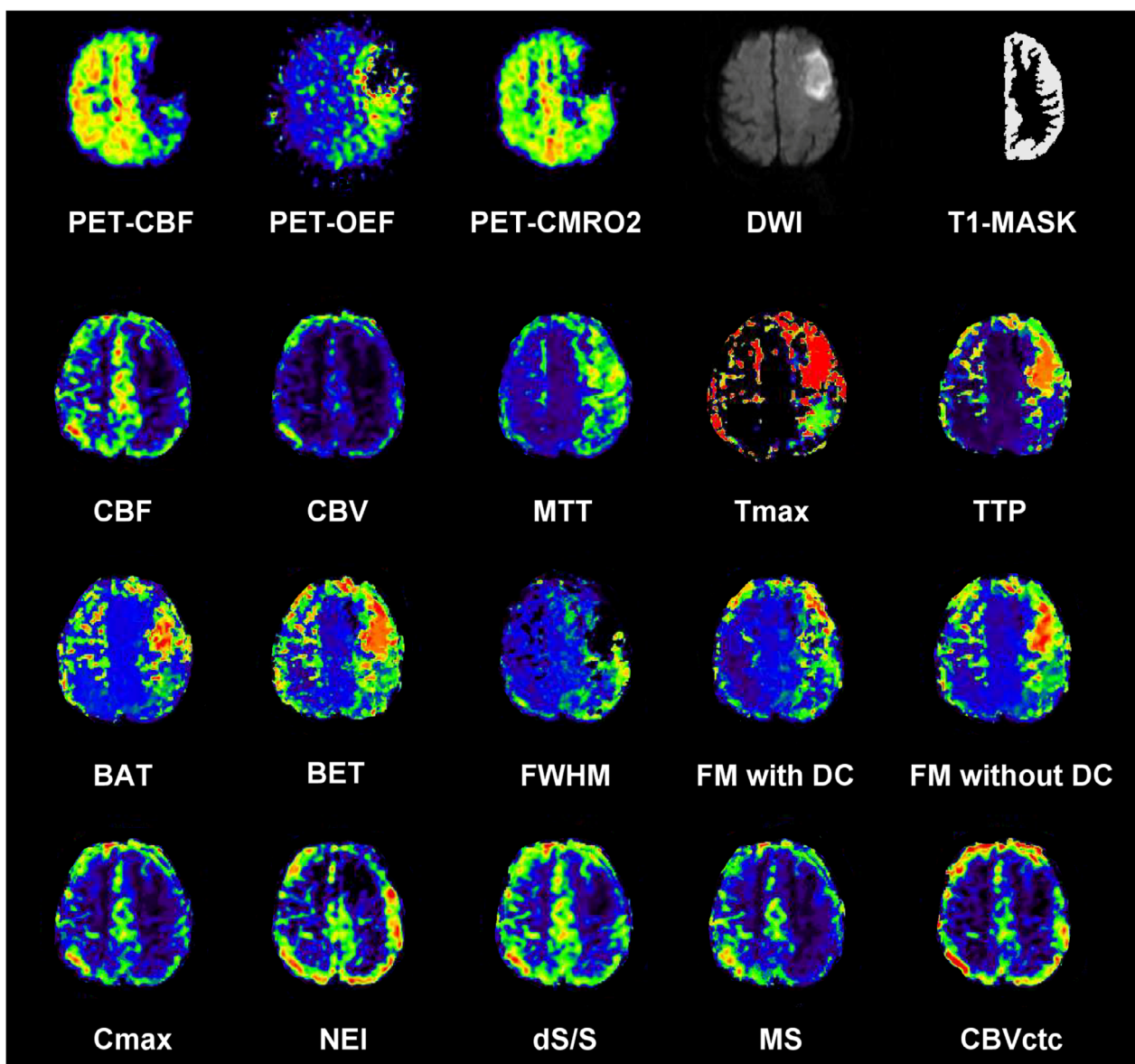


FIGURE 1: Voxel-based comparative analysis of positron emission tomography (PET)–cerebral blood flow (CBF), PET–oxygen extraction fraction (OEF), and PET–cerebral metabolic rate of oxygen (CMRO₂) with deconvolved perfusion-weighted imaging (PWI)–CBF, –cerebral blood volume (CBV), –mean transit time (MTT) and –time to maximum (Tmax) as well as nondeconvolved PWI–time to peak (TTP), –bolus arrival time (BAT), –bolus end time (BET), –full width at half maximum (FWHM), –first moment (FM), –maximum concentration (Cmax), –negative enhancement integral (NEI), –normalized signal drop (dS/S), –maximum slope (MS), and –CBV of the tissue contrast concentration time curve (CBV_{CTC}). Deconvolved PWI maps calculated by standard deconvolution with an arterial input function (AIF) from the tissue response curve. Nondeconvolved PWI maps calculated without deconvolution with an AIF. A T1-based grey matter mask was used for a voxel-based comparison of the PET and PWI maps. Ventricles, white matter, large arteries, sinuses, and areas of severely delayed contrast agent were excluded. receiver operating characteristic curve analysis was performed with a combination of the classic penumbra thresholds: PET-CBF < 20ml/100g/min, PET-OEF > mean OEF of unaffected hemisphere + 2 standard deviations and PET-CMRO₂ > 64μmol/100g/min. DC = delay correction; DWI = diffusion-weighted imaging.

below the minimum value of the individual contralateral OEF values (group A). The remaining voxels were used for further analysis.

For analysis of group A, we chose previously validated PET thresholds which fulfilled the classic criteria for penumbra with reduced CBF, compensatory increased OEF, and relatively preserved CMRO₂: (1) established CBF penumbra

threshold <20ml/100g/min,^{2,3,8} (2) significantly elevated OEF of more than the individual mean contralateral OEF plus 2 standard deviations (OEF > mean OEF_{contr} + 2 SD),³⁸ and (3) viable tissue threshold CMRO₂ > 64μmol/100g/min (equates to >1.5ml/100g/min).^{4,7,8,39} For analysis of group B, we chose the established PET-CBF penumbra threshold <20ml/100g/min.^{2,3,8}

Statistical Image Analysis

The accuracy of the PWI maps to detect the penumbral flow threshold as defined by full quantitative PET was determined by a receiver operating characteristic (ROC) curve analysis. The previously defined classic ^{15}O -PET-based penumbra criteria $\text{CBF} < 20\text{ml}/100\text{g}/\text{min}$, $\text{OEF} > \text{mean OEF}_{\text{contr}} + 2\text{SD}$, and $\text{CMRO}_2 > 64\mu\text{mol}/100\text{g}/\text{min}$ were used as a discriminator to define tissue as penumbral or nonpenumbral in group A. The established PET-CBF penumbra threshold of $<20\text{ml}/100\text{g}/\text{min}$ was used as a discriminator in group B. The ROC curve analysis provides 2 important measures, the area under the curve (AUC) and the equal sensitivity and specificity threshold (ESST)-based cutoff thresholds. The AUC represents a threshold independent accuracy measure of penumbral flow threshold detection. The ESST-based cutoff threshold represents the optimal threshold of the PWI maps to detect the penumbra threshold as defined by the stringent penumbral PET criteria. The ROC curve analysis was performed separately for each patient identifying the AUC and the ESST-based cutoff thresholds for each PWI map. The median and interquartile range (IQR) of the AUC and the median and bootstrapped confidence interval (CI) of the ESST-based cutoff thresholds as well as their sensitivity and specificity values were calculated. To test the ROC curve-derived optimal penumbral flow Tmax and TTP thresholds, we calculated bias-corrected and accelerated (BCa) bootstrapped 95% CIs (iterations = 1,000; random number seed = 978), adjusted for possible bias and skewness in the bootstrap distribution.⁴⁰

We tested for differences of PWI map performance (AUC) between the PW maps. The differences of the AUC were tested by a repeated-measures analysis of variance on ranks and a post hoc analysis Student–Newman–Keuls procedure for multiple comparisons at a corrected type I error level of 0.05. Data were analyzed with Sigmaplot 12.5 (Sysstat, 2012), R software (v3.5.0) and MedCalc (v18.11).

Results

Clinical Data

In this comparative study 2 groups were analyzed: group A (PET-CBF, -OEF, and - CMRO_2) included 10 patients (6 women, 4 men) with acute or subacute ischemic stroke (median age = 66 years [IQR = 56–74], median NIHSS = 12 [IQR = 4–14]). Consecutive PET and MRI were performed within 48 hours (median time = 10 hours [IQR = 4–35]) after stroke onset. Five patients were measured within 12 hours (time = 4 hours [IQR = 2.9–4.9]), and 5 patients measured between 12 to 48 hours (time = 35 hours [IQR = 17.8–42]). The median time delay between PET and MRI was 116 minutes (IQR = 100–150). Stenosis of the internal

carotid artery (ICA) or MCA was present in 6 patients ipsilateral and in 2 patients contralateral to the infarct (Table 1). Group B (PET-CBF) included 23 patients (12 women, 11 men) with acute or subacute ischemic stroke (median age = 56 years [IQR = 42–63], median NIHSS = 13 [IQR = 7–18]). Consecutive PET and MRI was performed within 48 hours (median time = 12 hours [IQR = 7–25]) after stroke onset. Ten patients were measured within 12 hours (time = 5.8 hours [IQR = 3.5–7]), and 13 patients were measured between 12 to 48 hours (time = 24 hours [IQR = 19.8–31.5]). The median time delay between PET and MRI was 67 minutes (IQR = 51–138). Stenosis of the ICA or MCA was present in 10 patients ipsilateral and in 4 patients contralateral to the infarct.

ROC Curve Analysis

All patients exhibited penumbral tissue on PET and PWI up to 48 hours after ischemic stroke (Fig 2). Accuracy of the PWI maps to detect penumbral tissue, as defined by the ROC curve analysis, varied considerably between the different maps and was best for deconvolved Tmax in group A and best for deconvolved Tmax and nondeconvolved TTP and FM without DC in group B. The ROC curve analysis was performed separately for each patient and PWI modality. The AUC values, which indicate the threshold independent performance to detect penumbral flow, were pooled among the 10 patients (group A) and 23 patients (group B) for every single PW map. The best performing PW map based on the AUC of the penumbra gold standard PET group (group A) was deconvolved Tmax (AUC = 0.88, IQR = 0.78–0.91), which performs significantly better ($p < 0.05$) than other established deconvolved PW maps, for example, CBF (AUC = 0.70, IQR = 0.64–0.85) and MTT (AUC = 0.69, IQR = 0.62–0.79) as well as nondeconvolved PW maps, for example, TTP (AUC = 0.83, IQR = 0.74–0.88) and FM without DC (AUC = 0.81, IQR = 0.74–0.87; Table 2).

The optimal pooled thresholds to detect penumbral flow based on the ESST of the penumbra gold standard PET group (group A) were for the best deconvolved measure Tmax > 5.6 seconds (95% CI = 4.6–6.1) with a sensitivity of 81% (IQR = 70–83%) and a specificity of 81% (IQR = 71–83%) and for the best nondeconvolved measures TTP > 3.8 seconds (95% CI = 3.7–4.4) with a sensitivity of 77% (IQR = 68–81%) and a specificity of 77% (IQR = 67–82%). In the bigger PET-CBF group (group B), the optimal penumbral flow thresholds were for deconvolved Tmax > 6.0 seconds (95% CI = 4.9–6.9) with a sensitivity of 87% (IQR = 80–91%) and a specificity of 87% (IQR = 80–91%) and for the best nondeconvolved measures TTP > 4.1 seconds (95% CI = 3.9–4.9) with a sensitivity of 85% (IQR = 77–90%) and a specificity of 85% (IQR = 77–90%; Table 3).

TABLE 1. Clinical Patient Data

Patient ID	Site	Age, yr/Sex	NIHSS	Stroke to Imaging, h	MRI to PET, min	ICA/MCA Stenosis Ipsilateral, %	ICA/MCA Stenosis Contralateral, %	DWI Lesion, cm ³	PET Penumbra, cm ³
1	MCA R	56/M	14	3	111	0	0	9.3	18.3
2	MCA R	76/F	1	2.5	210	100	0	10.1	186.7
3	MCA L	48/M	12	40	271	0	60	17.4	208.3
4	MCA L	47/F	4	6	120	100	0	7.7	10.9
5	MCA R	71/F	18	14	57	0	0	20.1	129.4
6	MCA L	56/M	12	4.5	150	100	0	96.2	145.0
7	MCA L	85/F	6	35	102	0	0	40.4	23.5
8	MCA R	74/F	4	4	100	60	0	25.0	47.7
9	MCA R	62/F	15	46	127	90	70	21.6	42.0
10	MCA L	70/M	14	19	100	100	0	24.8	164.1
Mean/median		65/66	10/12	17.4/10	135/116	—	—	—	—
Interquartile range		56–74	4–14	4–35	100–150	—	—	—	—
Minimum		47	1	2.5	57	—	—	—	—
Maximum		85	18	46	271	—	—	—	—

DWI = diffusion weighted lesions; F = female; ICA = internal carotid artery; ID = identification; L = left; M = male; MCA = middle cerebral artery; MRI = magnetic resonance imaging; NIHSS = National Institutes of Health Stroke Scale; PET = positron emission tomography; R = right.

Four representative ROC curves of the best PWI map T_{max} with the AUC values and the sensitivities and specificities at the optimal operating points where equal weights were attributed to sensitivity and specificity (ESST) are shown in Figure 3.

Discussion

This prospective imaging study of acute and subacute ischemic stroke was performed to improve mismatch-based tissue at risk detection and guide treatment decisions in ischemic stroke. To this end, we validated the whole range of established PW maps against full quantitative ¹⁵O-PET to determine the optimal PWI maps and thresholds to detect the penumbral flow threshold in ischemic stroke within 48 hours of symptom onset. The optimal PWI map and threshold that delineates penumbra from oligemia was identified using a voxel-based ROC curve analysis based on the classic PET penumbra definition of reduced blood flow (CBF) increased oxygen extraction (OEF) and stable oxygen metabolism (CMRO₂) in the gold standard PET group (group A) and the established PET penumbral flow threshold of reduced CBF in the larger PET group (group B).

Several novel findings, all with clear clinical implications, emerged from our gold standard PET group (group A) analysis: (1) the best PW parameter T_{max} had an excellent threshold independent prediction of penumbral flow (AUC = 0.88), (2) the optimal penumbral flow threshold of the most predictive PW map T_{max} > 5.6 seconds was highly accurate with a sensitivity and specificity above 80%, and (3) PW T_{max} was highly reliable to identify the penumbral flow threshold up to 48 hours after stroke onset.

The current study has new important implications for mismatch detection in acute stroke, and several main issues need to be discussed. The threshold independent performance of PW T_{max} was excellent with an AUC of 0.88. T_{max} significantly outperformed other deconvolved and nondeconvolved measures (group A). The bigger PET-CBF group validation (group B) provides evidence that T_{max}, TTP, and FM without DC are the best PWI parameters to detect the upper penumbral flow threshold. These results are roughly in line with those from the smaller full quantitative gold standard PET group (group A), which further strengthens the validity of our results and supports the use of deconvolved T_{max} and nondeconvolved TTP if no AIF is used. These results are important because previous

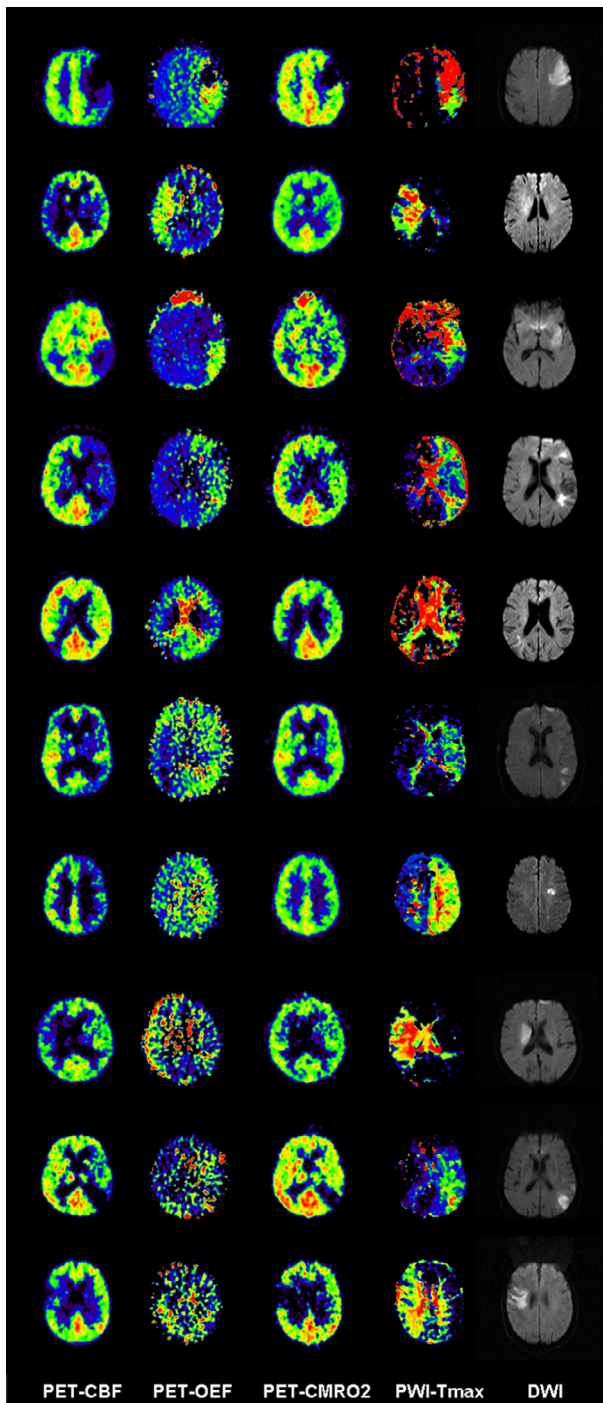


FIGURE 2: Coregistered images of multitracer ^{15}O - positron emission tomography (PET), magnetic resonance perfusion-weighted imaging (PWI) time to maximum (Tmax) and diffusion-weighted imaging (DWI) in all 10 patients (group A) with acute and subacute ischemic stroke. All patients show penumbral tissue on PET with reduced cerebral blood flow (CBF), elevated oxygen extraction fraction (OEF), and normal to reduced cerebral metabolic rate of oxygen (CMRO_2).

validation studies in acute stroke showed conflicting results concerning the best PW parameter and threshold. Most previous studies validated PWI maps against a single quantitative PET or Xe-CT penumbra threshold ($\text{CBF} <$

TABLE 2. Area under the Curve Values (Median) of Group A (PET-CBF, -OEF, - CMRO_2) and Group B (PET-CBF) for Deconvolved Tmax, CBF, CBV, MTT, and Nondeconvolved TTP, BAT, BET, FWHM, FM without/with DC, Cmax, MS, CBV_{CTC} , dS/S, and NEI

PW Maps	AUC, Group A	AUC, Group B
Tmax ^a	0.88 (0.78–0.91) ^a	0.94 (0.88–0.97) ^b
CBF	0.70 (0.64–0.85)	0.84 (0.81–0.88)
CBV	0.60 (0.56–0.67)	0.65 (0.57–0.66)
MTT	0.69 (0.62–0.79)	0.81 (0.79–0.89)
TTP	0.83 (0.74–0.88)	0.93 (0.85–0.96) ^b
BAT	0.69 (0.67–0.73)	0.82 (0.80–0.87)
BET	0.65 (0.57–0.73)	0.80 (0.71–0.84)
FWHM	0.61 (0.60–0.68)	0.65 (0.61–0.77)
FM without DC	0.81 (0.74–0.87)	0.89 (0.84–0.93) ^b
FM with DC	0.59 (0.57–0.71)	0.61 (0.57–0.73)
Cmax	0.66 (0.59–0.76)	0.82 (0.79–0.89)
MS	0.68 (0.59–0.72)	0.80 (0.77–0.83)
CBV_{CTC}	0.62 (0.56–0.74)	0.72 (0.60–0.80)
dS/S	0.65 (0.58–0.78)	0.67 (0.59–0.79)
NEI	0.64 (0.59–0.67)	0.66 (0.61–0.69)

Results are derived from the receiver operating characteristic curve analysis.

^aSignificantly higher AUC values within group A.

^bSignificantly higher AUC values within group B. Repeated measures analysis of variance on ranks and post hoc analysis Student-Newman-Keuls procedure for multiple comparisons at a corrected type I error level of 0.05. Median values of the AUC values. Variation is stated as interquartile range. AUC = area under the curve; BAT = bolus arrival time; BET = bolus end time; CBF = cerebral blood flow; CBV = cerebral blood volume; CBV_{CTC} = cerebral blood volume of the tissue contrast concentration time curve; Cmax = maximum of the concentration time curve; CMRO_2 = cerebral metabolic rate of oxygen; DC = delay correction; dS/S = normalized signal drop; FM = first moment; FWHM = full width at half maximum; MS = maximum slope; MTT = mean transit time; NEI = negative enhancement integral; OEF = oxygen extraction fraction; PET = positron emission tomography; PW = perfusion weighted; Tmax = time to maximum; TTP = time to peak.

20ml/100g/min). However, since the mismatch concept is a surrogate of the classic penumbra definition by PET,^{2,3} our study was particularly suitable to determine the best PW parameter to detect penumbra as defined by full quantitative PET. One reason why deconvolved Tmax detects the penumbral flow threshold with such a high accuracy might be the deconvolution procedure used for quantification, which, from a theoretical point of view, has advantages over

TABLE 3. Optimal Penumbra Flow Threshold Values (Median) of Group A (PET-CBF, -OEF, -CMRO₂) and Group B (PET-CBF) for the Best Deconvolved Tmax and Nondeconvolved TTP Perfusion Maps

PW Maps	PF Threshold, s ^a	Sensitivity, %	Specificity, %
Group A			
Tmax	>5.6 (95% CI = 4.6–6.1)	81 (IQR = 70–83)	81 (IQR = 71–83)
TTP	>3.8 (95% CI = 3.7–4.4)	77 (IQR = 68–81)	77 (IQR = 67–82)
Group B			
Tmax	>6.0 (95% CI = 4.9–6.9)	87 (IQR = 80–91)	87 (IQR = 80–91)
TTP	>4.1 (95% CI = 3.9–4.9)	85 (IQR = 77–90)	85 (IQR = 77–90)

Results are derived from the receiver operating characteristic curve analysis. PF threshold is defined by the ESST.

^aBC_a bootstrap 95% CI (1,000 iterations; random number seed = 978).

CBF = cerebral blood flow; CI = confidence interval; CMRO₂ = cerebral metabolic rate of oxygen; ESST = penumbra flow threshold corresponding to the equal sensitivity and specificity threshold; OEF = oxygen extraction fraction; PET = positron emission tomography; PF threshold = optimal penumbra flow threshold; PW = perfusion weighted; Tmax = time to maximum; TTP = time to peak.

nondeconvolved measures (eg, TTP, FM). Deconvolution might therefore help to detect tissue that is affected by not only low blood flow but also compromised oxygen metabolism. For a thorough discussion of deconvolution, see Reimer and colleagues.¹⁸ Tmax performs better than physiologic PW maps because Tmax calculation is only dependent on the tissue response curve to its peak and not on the whole response curve like many other maps (eg, CBV, MTT, FM), making Tmax also less prone to artifacts.^{19,35} The accuracy to detect penumbra flow thresholds with PW measures shows slightly lower AUC values if validated against the classical PET definition of penumbra (group A) rather than against a single PET penumbra CBF threshold (group B; Tmax AUC = 0.88 vs 0.94). This might be attributed to PWI being a surrogate of blood flow, and a direct comparison to PET-based blood flow without metabolic measures is more straightforward. However, our validation based on full quantitative PET (group A) might well provide a more accurate performance of PWI penumbra flow detection.

The optimal penumbra threshold to distinguish penumbra from oligemic tissue is Tmax > 5.6 seconds. Along with the optimal thresholds for TTP > 3.8 seconds, our results are in line with the results of group B and some previous comparative PET-, Xe-CT-, and MR-based studies.^{19,36,41} However, we found a slightly lower optimal TTP threshold than some previous studies.^{19,36,42,43} This might be due to the classic PET definition of penumbra used for PWI validation leading to further improved optimal penumbra thresholds. We also performed a voxelwise ROC curve analysis rather than a ROI-based analysis, which might lead to less biased thresholds.

Because patients in this study exhibited penumbra tissue up to 48 hours after stroke onset, we could prove

for the first time that the performance of the PWI parameter Tmax > 5.6 seconds is excellent in detecting the upper penumbra flow threshold up to 48 hours after stroke onset. This time window is in line with previous PET-based studies, which detected penumbra tissue with ¹⁵O-PET as late as 18 to 48 hours^{4,10} and with ¹⁸F-fluoromisonidazole PET as late as 48 hours.⁴⁴

Few previous studies have validated the mismatch concept in acute and subacute ischemic stroke. There have been 2 different approaches to validate the performance of established PWI maps to detect penumbra flow: MR-based validation studies compare PWI maps with infarct growth on late MRI as a reference in patients without reperfusion. These studies either compare the performance of different PWI maps^{35,45,46} or identify the optimal perfusion threshold of a single PWI map^{43,47} to detect penumbra tissue. It is crucial in these MR-based validations to exclude reperfusers. Therefore, these studies only included patients without thrombolytic therapy^{43,45,47,48} or patients with proven nonreperfusion.³⁵ In addition, the optimal imaging method and time to accurately detect the final infarct is of importance.⁴⁹ These studies investigated different PWI maps and found different results in terms of the best PWI map and threshold to detect tissue at risk of infarction. Some variation in results might be explained by methodological differences of how reperfusers were excluded and how final infarct was defined.

PET or Xe-CT-based studies compare PWI maps back to back with a measure of quantitative CBF, for example, PET^{19,36,42} or Xe-CT.⁴¹ In these studies, the best PWI maps and thresholds are validated against CBF < 20ml/100g/min, which is used to discriminate oligemic from penumbra tissue.^{2,3} Previous studies of our group^{19,22,23,42} found

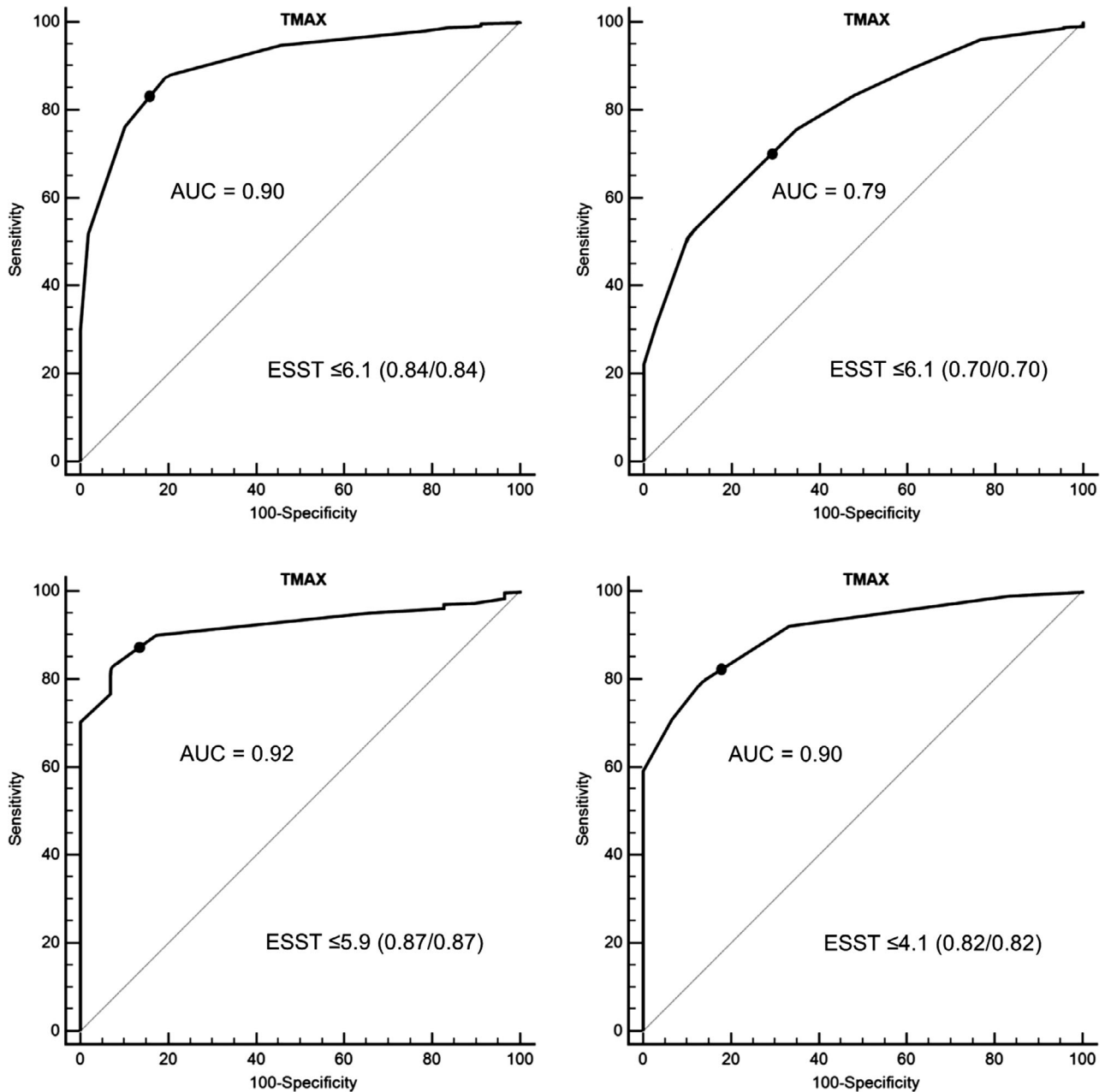


FIGURE 3: Representative receiver operating characteristic curves of 4 patients illustrating the performance of time to maximum (Tmax) with respect to penumbral flow detection based on full quantitative positron emission tomography (PET)–cerebral blood flow, PET–oxygen extraction fraction, and cerebral metabolic rate of oxygen. The equal sensitivity and specificity threshold (ESST) is marked on the receiver operating characteristic curve. The corresponding optimal penumbral flow threshold with its sensitivity and specificity is shown. AUC = area under the curve.

deconvolved Tmax > 6.1 seconds and nondeconvolved TTP > 4.2 seconds, Cmax < 0.66, and FM without DC > 3.6 seconds to perform best and equally well in discriminating tissue with PET CBF < 20ml/100g/min. However, these studies did not validate PW maps against penumbra as defined by full quantitative ¹⁵O-PET. Another study of 5 acute and subacute stroke patients investigated the performance of PW maps (Tmax > 5.5 seconds, MTT > 6 seconds, TTP > 4.8 seconds) to detect penumbral flow thresholds against quantitative and full quantitative ¹⁵O-PET and found no difference in

performance.³⁶ Olivot and colleagues⁴¹ validated Tmax and MTT in 7 subacute stroke patients against Xe-CT and found Tmax > 4 seconds to be more reliable than MTT > 10 seconds to detect critical hypoperfusion.

In summary, previous MR-, PET- and Xe-CT-based validation studies found conflicting results as to which PW map and threshold performs best in detecting penumbral tissue. To settle the dispute, we validated all established PW maps against the classical penumbra definition of full quantitative PET up to 48 hours after stroke and provide

clear recommendations to the clinician in terms of the best PW map and its optimal threshold.

From a clinical point of view, these results are important because the optimal PW maps and penumbra thresholds validated against full quantitative PET up to 48 hours of stroke onset are pivotal to detect penumbral tissue and can help the clinician to decide on revascularization or other options of treatment in acute stroke beyond the established time windows. This is particularly true because recent clinical stroke studies (DEFUSE-3 and DAWN)^{16,17} have shown a clinical benefit of endovascular revascularization based on mismatch detection within 24 hours of stroke onset.

Several methodological issues need to be discussed. First, we validated the whole range of PW maps against full quantitative ¹⁵O-PET and processed these maps with a validated software (PMA) which allows calculation of a wide range of deconvolved and nondeconvolved PW maps with high precision.³¹ Second, our validation was performed using a voxel-based ROC-curve analysis, which allows an unbiased approach to detect the most predictive PW maps and their optimal thresholds.³⁵ Third, because we wanted the sensitivity and specificity to be equal for optimal penumbral flow threshold definition, the best cut-off threshold using the ROC curve analysis was determined by the ESST.³⁵ However, depending on the individual clinical setting, a higher sensitivity or specificity might be required and the optimal threshold values might be different. Fourth, the PWI-based penumbral flow thresholds are valid for grey matter only, and the inclusion of white matter may lead to slightly higher (eg, Tmax) or lower (eg, CBF) PWI penumbra thresholds. We minimized this error by creating a grey matter mask that excluded white matter voxels. Therefore, the results are not applicable to pure subcortical infarcts. Fifth, we validate the upper limit of penumbral flow (ie, discrimination of penumbral from oligemic flow). This is a standard approach,^{35,36,41} because the lower limit of penumbral flow (ie, the infarct core threshold) is defined by the DWI lesion within the mismatch concept and has previously been validated by ¹¹C-flumazenil PET.^{50,51} Sixth, we present the biggest patient sample of full quantitative ¹⁵O-PET with consecutive PW MR in acute stroke. The restricted numbers in the literature are due to the very challenging logistics to perform these measures in acute stroke (see Patients and Methods section). However, our bigger PET-CBF group validation (group B) shows time-driven parameters to perform best, which strengthens the results of the gold standard PET group (group A). Seventh, the time of stroke onset to imaging does not influence the validity of our results because the upper CBF “penumbra” threshold is, unlike the lower CBF “infarction” threshold, not time

dependent.^{1,52} Eighth, the brief inhalation ¹⁵O-PET method used in this study can be used for full quantitative regional measurement of CBF, OEF, and CMRO₂. It has been fully validated for a wide range of values and is valid for low blood flow values under pathologic conditions such as stroke.^{25,53} The main advantage of the brief inhalation method is that it is a rapid technique, is easy to repeat, and involves a lower radiation dosage. It is less time consuming than the steady-state ¹⁵O-PET method, and less patient cooperation is needed, which is, along with the shorter scanning procedure, an advantage in stroke patients.⁵⁴ Ninth, flow and metabolic changes during consecutive MR and PET imaging were minimized by keeping the time between both imaging modalities as short as possible, excluding patients with revascularization treatment and clinical changes (NIHSS > 2 points) during and between imaging. We also monitored CBF by sonography of the cerebral arteries before and between the scans. However, to eliminate changes between MR and PET completely, imaging should be performed simultaneously on a PET/MR hybrid scanner in future studies. Tenth, PWI maps showed an individual variation of the optimal penumbral flow threshold despite the use of deconvolution algorithms based on input functions in deconvolved PWI or normalization to the contralateral nonaffected hemisphere in nondeconvolved PWI. The use of quantitative bookend DSC-MR in future studies might reduce this individual over- or underestimation of penumbral tissue.⁵⁵ Eleventh, because the classical PET-based definition of penumbra is based on CBF, OEF, and CMRO₂, mismatch-based penumbral tissue detection in acute stroke might benefit from additional validated MR-based quantitative measures of OEF and oxygen metabolism (CMRO₂).⁵⁶

In summary, this study of acute and subacute ischemic stroke validated a wide range of established PW parameters against the classical definition of penumbra as defined by full quantitative ¹⁵O-PET within 48 hours of stroke onset. We demonstrated that Tmax > 5.6 seconds is outstanding in detecting the upper penumbral flow threshold up to 48 hours after stroke onset and outperforms other PWI parameters. However, if no selection of an AIF is feasible, nondeconvolved TTP > 3.8 seconds is a very good alternative to Tmax. These results might help to expand acute stroke treatment well beyond the current time windows.

Acknowledgment

The research leading to these results received funding from the Max Planck Society and the Boll Foundation. This work was also funded by the Center for Stroke Research Berlin grant (01EO 0801 and 01EO 01301)

from the German Federal Ministry of Education and Research. The funding bodies had no role in study design, data collection and analysis, decision to publish, or preparation of the manuscript.

We thank the members of the neurocritical care unit (Department of Neurology), the staff of the MRI facility (Department of Neuroradiology), and especially the staff of the PET unit (Max-Planck-Institute for Neurological Research) for helpful cooperation in this multimodal imaging study.

Author Contributions

O.Z.W., H.F., L.R., and W.D.H. contributed to the study concept and design. O.Z.W., H.F., L.R., A.S., and W.M.H. contributed to data acquisition and analysis. O.Z.W., H.F., and L.R. contributed to drafting of the manuscript and figures. All authors revised the manuscript critically for important intellectual content and approved the final version.

Potential Conflicts of Interest

Nothing to report.

References

- Astrup J, Siesjo BK, Symon L. Thresholds in cerebral ischemia — the ischemic penumbra. *Stroke* 1981;12:723–725.
- Baron JC. Mapping the ischaemic penumbra with PET: implications for acute stroke treatment. *Cerebrovasc Dis* 1999;9:193–201.
- Heiss WD. Ischemic penumbra: evidence from functional imaging in man. *J Cereb Blood Flow Metab* 2000;20:1276–1293.
- Heiss WD, Huber M, Fink GR, et al. Progressive derangement of peri-infarct viable tissue in ischemic stroke. *J Cereb Blood Flow Metab* 1992;12:193–203.
- Hossmann KA. Viability thresholds and the penumbra of focal ischemia. *Ann Neurol* 1994;36:557–565.
- Ackerman RH, Correia JA, Alpert NM, et al. Positron imaging in ischemic stroke disease using compounds labeled with oxygen 15. Initial results of clinicophysiological correlations. *Arch Neurol* 1981;38:537–543.
- Lenzi GL, Frackowiak RS, Jones T. Cerebral oxygen metabolism and blood flow in human cerebral ischemic infarction. *J Cereb Blood Flow Metab* 1982;2:321–335.
- Powers WJ, Grubb RL Jr, Darriet D, Raichle ME. Cerebral blood flow and cerebral metabolic rate of oxygen requirements for cerebral function and viability in humans. *J Cereb Blood Flow Metab* 1985;5:600–608.
- Wise RJ, Bernardi S, Frackowiak RS, Legg NJ, Jones T. Serial observations on the pathophysiology of acute stroke. The transition from ischaemia to infarction as reflected in regional oxygen extraction. *Brain* 1983;106(pt 1):197–222.
- Marchal G, Beaudouin V, Rioux P, et al. Prolonged persistence of substantial volumes of potentially viable brain tissue after stroke: a correlative PET-CT study with voxel-based data analysis. *Stroke* 1996;27:599–606.
- Baron JC, Bousser MG, Comar D, Soussaline F, Castaigne P. Noninvasive tomographic study of cerebral blood flow and oxygen metabolism in vivo. Potentials, limitations, and clinical applications in cerebral ischemic disorders. *Eur Neurol* 1981;20:273–284.
- Warach S, Dashe JF, Edelman RR. Clinical outcome in ischemic stroke predicted by early diffusion-weighted and perfusion magnetic resonance imaging: a preliminary analysis. *J Cereb Blood Flow Metab* 1996;16:53–59.
- Sorensen AG, Buonanno FS, Gonzalez RG, et al. Hyperacute stroke: evaluation with combined multisection diffusion-weighted and hemodynamically weighted echo-planar MR imaging. *Radiology* 1996;199:391–401.
- Schlaug G, Benfield A, Baird AE, et al. The ischemic penumbra: operationally defined by diffusion and perfusion MRI. *Neurology* 1999;53:1528–1537.
- Sobesky J. Refining the mismatch concept in acute stroke: lessons learned from PET and MRI. *J Cereb Blood Flow Metab* 2012;32:1416–1425.
- Albers GW, Marks MP, Kemp S, et al. Thrombectomy for stroke at 6 to 16 hours with selection by perfusion imaging. *N Engl J Med* 2018;378:708–718.
- Nogueira RG, Jadhav AP, Haussen DC, et al. Thrombectomy 6 to 24 hours after stroke with a mismatch between deficit and infarct. *N Engl J Med* 2018;378:11–21.
- Reimer J, Montag C, Schuster A, et al. Is Perfusion MRI without deconvolution reliable for mismatch detection in acute stroke? Validation with 15O-positron emission tomography. *Cerebrovasc Dis* 2018;46:16–23.
- Zaro-Weber O, Moeller-Hartmann W, Siegmund D, et al. MRI-based mismatch detection in acute ischemic stroke: optimal PWI maps and thresholds validated with PET. *J Cereb Blood Flow Metab* 2017;37:3176–3183.
- Zaro-Weber O, Livne M, Martin SZ, et al. Comparison of the 2 most popular deconvolution techniques for the detection of penumbral flow in acute stroke. *Stroke* 2015;46:2795–2799.
- Zaro-Weber O, Moeller-Hartmann W, Heiss WD, Sobesky J. Influence of the arterial input function on absolute and relative perfusion-weighted imaging penumbral flow detection: a validation with 15O-water positron emission tomography. *Stroke* 2012;43:378–385.
- Zaro-Weber O, Moeller-Hartmann W, Heiss WD, Sobesky J. The performance of MRI-based cerebral blood flow measurements in acute and subacute stroke compared with 15O-water positron emission tomography: identification of penumbral flow. *Stroke* 2009;40:2413–2421.
- Zaro-Weber O, Moeller-Hartmann W, Heiss WD, Sobesky J. Maps of time to maximum and time to peak for mismatch definition in clinical stroke studies validated with positron emission tomography. *Stroke* 2010;41:2817–2821.
- Wienhard K, Dahlbom M, Eriksson L, et al. The ECAT EXACT HR: performance of a new high resolution positron scanner. *J Comput Assist Tomogr* 1994;18:110–118.
- Mintun MA, Raichle ME, Martin WR, Herscovitch P. Brain oxygen utilization measured with O-15 radiotracers and positron emission tomography. *J Nucl Med* 1984;25:177–187.
- Raichle ME, Martin WR, Herscovitch P, Mintun MA, Markham J. Brain blood flow measured with intravenous H₂(15)O. II. Implementation and validation. *J Nucl Med* 1983;24:790–798.
- Martin WR, Powers WJ, Raichle ME. Cerebral blood volume measured with inhaled C¹⁵O and positron emission tomography. *J Cereb Blood Flow Metab* 1987;7:421–426.
- Eriksson L, Holte S, Bohm C, Kesselberg M, Hovander B. Automated blood sampling system for positron emission tomography. *IEEE Trans Nucl Sci* 1988;35:703–707.

29. Sobesky J, Zaro-Weber O, Lehnhardt FG, et al. Does the mismatch match the penumbra? Magnetic resonance imaging and positron emission tomography in early ischemic stroke. *Stroke* 2005;36:980–985.
30. Cizek J, Herholz K, Vollmar S, Schrader R, Klein J, Heiss WD. Fast and robust registration of PET and MR images of human brain. *Neuroimage* 2004;22:434–442.
31. Kudo K, Christensen S, Sasaki M, et al. Accuracy and reliability assessment of CT and MR perfusion analysis software using a digital phantom. *Radiology* 2013;267:201–211.
32. Ostergaard L, Weisskoff RM, Chesler DA, Gyldensted C, Rosen BR. High resolution measurement of cerebral blood flow using intravascular tracer bolus passages. Part I: Mathematical approach and statistical analysis. *Magn Reson Med* 1996;36:715–725.
33. Leiva-Salinas C, Provenzale JM, Kudo K, Sasaki M, Wintermark M. The alphabet soup of perfusion CT and MR imaging: terminology revisited and clarified in five questions. *Neuroradiology* 2012;54:907–918.
34. Perthen JE, Calamante F, Gadian DG, Connelly A. Is quantification of bolus tracking MRI reliable without deconvolution? *Magn Reson Med* 2002;47:61–67.
35. Christensen S, Mouridsen K, Wu O, et al. Comparison of 10 perfusion MRI parameters in 97 sub-6-hour stroke patients using voxel-based perfusion operating characteristics analysis. *Stroke* 2009;40:2055–2061.
36. Takasawa M, Jones PS, Guadagno JV, et al. How reliable is perfusion MR in acute stroke? Validation and determination of the penumbra threshold against quantitative PET. *Stroke* 2008;39:870–877.
37. Butcher KS, Parsons M, MacGregor L, et al. Refining the perfusion-diffusion mismatch hypothesis. *Stroke* 2005;36:1153–1159.
38. Furlan M, Marchal G, Viader F, Derlon JM, Baron JC. Spontaneous neurological recovery after stroke and the fate of the ischemic penumbra. *Ann Neurol* 1996;40:216–226.
39. Baron JC, Rougemont D, Soussaline F, et al. Local interrelationships of cerebral oxygen consumption and glucose utilization in normal subjects and in ischemic stroke patients: a positron tomography study. *J Cereb Blood Flow Metab* 1984;4:140–149.
40. Efron B. Better bootstrap confidence intervals. *Journal of the American Statistical Association* 1987;82(397):171–185.
41. Olivot JM, Mlynash M, Zaharchuk G, et al. Perfusion MRI (Tmax and MTT) correlation with xenon CT cerebral blood flow in stroke patients. *Neurology* 2009;72:1140–1145.
42. Sobesky J, Zaro-Weber O, Lehnhardt FG, et al. Which time-to-peak threshold best identifies penumbral flow? A comparison of perfusion-weighted magnetic resonance imaging and positron emission tomography in acute ischemic stroke. *Stroke* 2004;35:2843–2847.
43. Neumann-Haefelin T, Wittsack HJ, Wenserski F, et al. Diffusion- and perfusion-weighted MRI. The DWI/PWI mismatch region in acute stroke. *Stroke* 1999;30:1591–1597.
44. Read SJ, Hirano T, Abbott DF, et al. Identifying hypoxic tissue after acute ischemic stroke using PET and 18F-fluoromisonidazole. *Neurology* 1998;51:1617–1621.
45. Grandin CB, Duprez TP, Smith AM, et al. Which MR-derived perfusion parameters are the best predictors of infarct growth in hyperacute stroke? Comparative study between relative and quantitative measurements. *Radiology* 2002;223:361–370.
46. Rohl L, Geday J, Ostergaard L, et al. Correlation between diffusion- and perfusion-weighted MRI and neurological deficit measured by the Scandinavian Stroke Scale and Barthel Index in hyperacute subcortical stroke (< or = 6 hours). *Cerebrovasc Dis* 2001;12:203–213.
47. Parsons MW, Yang Q, Barber PA, et al. Perfusion magnetic resonance imaging maps in hyperacute stroke: relative cerebral blood flow most accurately identifies tissue destined to infarct. *Stroke* 2001;32:1581–1587.
48. Rohl L, Ostergaard L, Simonsen CZ, et al. Viability thresholds of ischemic penumbra of hyperacute stroke defined by perfusion-weighted MRI and apparent diffusion coefficient. *Stroke* 2001;32:1140–1146.
49. Lansberg MG, O'Brien MW, Tong DC, Moseley ME, Albers GW. Evolution of cerebral infarct volume assessed by diffusion-weighted magnetic resonance imaging. *Arch Neurol* 2001;58:613–617.
50. Heiss WD, Sobesky J, Smekal U, et al. Probability of cortical infarction predicted by flumazenil binding and diffusion-weighted imaging signal intensity: a comparative positron emission tomography/magnetic resonance imaging study in early ischemic stroke. *Stroke* 2004;35:1892–1898.
51. Guadagno JV, Warburton EA, Jones PS, et al. How affected is oxygen metabolism in DWI lesions?: A combined acute stroke PET-MR study. *Neurology* 2006;67:824–829.
52. Jones TH, Morawetz RB, Crowell RM, et al. Thresholds of focal cerebral ischemia in awake monkeys. *J Neurosurg* 1981;54:773–782.
53. Altman DI, Lich LL, Powers WJ. Brief inhalation method to measure cerebral oxygen extraction fraction with PET: accuracy determination under pathologic conditions. *J Nucl Med* 1991;32:1738–1741.
54. Baron JC, Frackowiak RS, Herholz K, et al. Use of PET methods for measurement of cerebral energy metabolism and hemodynamics in cerebrovascular disease. *J Cereb Blood Flow Metab* 1989;9:723–742.
55. Srouf JM, Shin W, Shah S, Sen A, Carroll TJ. SCALE-PWI: a pulse sequence for absolute quantitative cerebral perfusion imaging. *J Cereb Blood Flow Metab* 2011;31:1272–1282.
56. Lin W, Powers WJ. Oxygen metabolism in acute ischemic stroke. *J Cereb Blood Flow Metab* 2018;38:1481–1499.